

Sorption, Dilation, and Partial Molar Volumes of Carbon Dioxide and Ethane in Cross-Linked Poly(ethylene oxide)

Cláudio P. Ribeiro, Jr., and Benny D. Freeman*

Center for Energy and Environmental Resources, The University of Texas at Austin,
10100 Burnet Road, Building 133, Austin, Texas 78758

Received July 2, 2008; Revised Manuscript Received September 11, 2008

ABSTRACT: Experimental gas solubility and sorptive dilation data are reported for carbon dioxide and ethane in a cross-linked poly(ethylene oxide) rubber prepared by photopolymerization of poly(ethylene glycol)diacrylate. Five different operating temperatures ($253 \leq T \text{ (K)} \leq 308$) were considered, with a maximum gas pressure of 2.16 MPa (21.3 atm). The importance of taking sorptive dilation into account in the determination of gas solubility in polymers by the pressure–decay method was demonstrated. Sorption isotherms in terms of gas fugacity were described by the Flory–Huggins model. In the case of ethane, the Flory–Huggins interaction parameter was a decreasing function of temperature. In contrast, for carbon dioxide, a single parameter represented all isotherms. Dilation and sorption data were combined to calculate the partial molar volume (PMV) of the gases in the polymer, which was an increasing function of temperature. The PMV data were compared to the available literature data for other rubbery polymers and liquids. The chemical structure of the polymer influenced the PMV of the sorbed gas, and a correlation between matrix (i.e., solvent or polymer) solubility parameter and PMV was found.

1. Introduction

The removal of carbon dioxide from mixtures with light gases is an important industrial separation. First, carbon dioxide is a common impurity in natural gas that must be removed for heating value improvement. In the United States alone, the mean production of natural gas between 2000 and 2005 surpassed 535 billion m^3 (STP, dry gas),¹ and about 20% of this gas contains CO_2 at concentrations higher than the allowable U.S. pipeline specification (2 vol % or less).² Furthermore, most hydrogen in the U.S., whose current demand reaches about 9 million tons per year,³ and about one-half of the world's hydrogen supply, is produced by steam reforming of natural gas, with CO_2 as a byproduct. Another important aspect is the control of global warming and climate change. Overall, as a result of human activity, about 7 Gton of carbon is emitted to the atmosphere each year,⁴ a large portion of which is CO_2 .

Currently, CO_2 removal from gas mixtures is mainly achieved by absorption in amine solutions.⁵ Despite its widespread application, this technology is associated with high energy consumption and operating costs.⁶ In addition, it may present some operating problems such as flooding, excessive foam formation, and liquid entrainment.⁷ Therefore, a number of alternatives have been investigated in the literature to perform CO_2 separation, including adsorption, hydrate formation, electrochemical pumps, cryogenic distillation, and membrane separation.^{4,8}

Membrane processes, in particular, can offer many advantages over traditional amine-based systems, such as higher flexibility, reduced energy requirement, ease of process integration, lower capital and operating costs, and smaller footprint.^{5,6} In the specific case of natural gas treatment, membrane plants have already been installed for small gas flow rates. However, the flux of current commercial membranes, based on cellulose acetate and polyimides, is considered to be too low, and, due to plasticization by carbon dioxide and higher hydrocarbons, their selectivity is often not high enough to compete with amine systems for medium and large gas flow rates, which account for more than 99% of the total market.⁷ As a result, the

development of improved membrane materials to remove CO_2 from light gases has been the subject of intense research,^{9–11} and cross-linked poly(ethylene oxide)s (XLPEOs) have recently emerged as a potential alternative membrane material.^{12–16}

These rubbery materials can be obtained by either photopolymerization^{12,15,16} or chemical cross-linking^{13,14} of acrylate-functionalized low molecular-weight poly(ethylene oxide) oligomers such as poly(ethylene glycol)diacrylate (PEGDA). They work as solubility-selective membranes, with high permeability and selectivity for CO_2 on account of the specific interactions of this acid gas with the ether groups in the polymeric chain.^{17,18} Although these interactions have been known for a long time, high molecular weight PEO is semicrystalline at ambient conditions, which is deleterious for gas permeability.¹⁷ The short nature of the runs of ethylene oxide in these XLPEO materials, combined with cross-linking, successfully suppresses crystallinity.^{15,16,18}

Most studies concerning XLPEOs so far have focused on the pure gas permeation properties of dense films prepared from both pure acrylate-functionalized oligomers^{13,14,19–22} and their binary mixtures.^{12,15,16,22–25} A central focus of these studies has been developing correlations between permeation properties and the architecture of the polymer network, as well as understanding the influence of operating parameters such as feed gas fugacity and temperature on membrane performance.

Despite the fact that the resulting membranes are solubility-selective, much less attention has been devoted to the experimental measurement of gas sorption by XLPEOs. Some solubility data are available for CO_2 and a few hydrocarbons (C_1 to C_3) at 308 K in materials synthesized from PEGDA,²⁰ poly(propylene glycol) diacrylate,²¹ and different mixtures of PEGDA and poly(ethylene glycol) methyl ether acrylate (PEGMEA).²⁴ Apparently, the only systematic studies of gas and vapor solubility were those of Lin and Freeman,²⁶ who determined sorption isotherms for CO_2 and five hydrocarbons in a PEGDA-based rubber at five temperatures ranging from 253 to 308 K, and Kelman et al.,²⁷ who reported sorption isotherms for CO_2 and ethane in a PEGDA–PEGMEA copolymer at three different temperatures. Because no information regarding the sorptive dilation of XLPEOs is available in the literature, all of these solubility data were obtained neglecting

* Corresponding author. Phone: (512) 232-2803. Fax: (512) 232-2807. E-mail: freeman@cche.utexas.edu.

the effect of polymer dilation, which can lead to some error in solubility because experimental methods for measuring gas solubility in polymers are sensitive to the volume of the polymer sample,^{28,29} which increases as gas sorbs into the polymer.

Therefore, in the present study, pure gas dilation and sorption data for carbon dioxide and ethane in a XLPEO material prepared by photopolymerization of PEGDA are reported. Ethane was chosen as the model hydrocarbon because, apart from being one of the major components of natural gas, it forms a maximum pressure azeotrope with CO₂ that can complicate effective natural gas treatment.^{30,31} Five different operating temperatures ($253 \leq T \text{ (K)} \leq 308$) were considered, with a maximum gas pressure of 2.16 MPa (21.3 atm). Dilation and sorption data were combined and used to determine Flory–Huggins interaction parameters and partial molar volumes (PMV) for each gas in the polymer. A database of PMV values for these two gases in liquids and rubbery polymers was constructed, and a correlation between PMV and solubility parameter was observed, so the chemical structure of the polymer can influence the PMV of the sorbed gas.

2. Experimental Section

2.1. Materials and Polymer Preparation. Cylinders of ethane (99% purity) and carbon dioxide (99.999% purity) were purchased from Airgas Southwest Inc. (Corpus Christi, TX). Poly(ethylene glycol) diacrylate (PEGDA; nominal MW 700 g/mol) and 1-hydroxyl-cyclohexyl phenyl ketone (HCPK; 99% purity), the photoinitiator, were obtained from Aldrich Chemical Co. (Milwaukee, WI). All gases and chemicals were used as received.

The XLPEO films were prepared by adding 0.1 wt % HCPK to pure PEGDA and stirring the resulting mixture for at least 2 h. The resulting solution was sandwiched between two quartz plates separated by stainless steel spacers to control film thickness. The solution was polymerized by exposure to 312 nm UV light for 90 s at 3 mW/cm² in a UV cross-linker (Fisher Scientific, model FB-UVXL-1000). These UV exposure conditions were chosen on the basis of previous studies, which provided FTIR spectroscopy evidence of complete conversion of the acrylate groups.^{20,21} The solid film thus obtained was immersed in an ethanol bath for 3 days to remove any residual components or low-molecular-weight species, and then it was dried at room temperature for at least 7 days. The liquid bath was replaced daily with fresh ethanol. The final film thickness, measured with a digital micrometer (Mitutoyo, model ID-C112E) readable to $\pm 1 \mu\text{m}$, was 300 μm . At 23 °C, the density of the XLPEO film was $(1.1822 \pm 0.0007) \text{ g/cm}^3$, a value determined on the basis of the difference between the weight of a polymer sample in air and in *n*-heptane. According to Lin et al.,²⁴ the glass transition temperature of this material is 233 K.

2.2. Dilation Measurements. The dilation experiments were performed in the same apparatus adopted by Raharjo et al.³² in their study with PDMS and hydrocarbons. A strip of the polymer, 73.6 mm in length at 23 °C, was placed in the sample holder, and an L-shaped wire was hung at its end, as shown in Figure 1. The sample holder was placed inside a Jerguson gauge, and the position of the L-shaped wire was monitored by a COHU (model 4915-2000) CCD camera (San Diego, CA). At the beginning of each run, the distance L_0 between the end of the L-shaped wire and the reference wire was measured under vacuum at the operating temperature. A given amount of gas was allowed into the chamber, and digital pictures were periodically taken to determine the position of the L-shape wire as a function of time. Details regarding the image analysis protocol are given elsewhere.³³ Once equilibrium was reached, which could take from 120 min to 7 days depending on the operating temperature and on the gas under study, the new distance L_1 associated with pressure P_1 was measured, and the corresponding increase in the polymer volume (ΔV) was computed assuming isotropic dilation:

$$\frac{\Delta V}{V_0} = \frac{V - V_0}{V_0} = \left(1 + \frac{L_1 - L_0}{l_0}\right)^3 - 1 \quad (1)$$

where l_0 is the length of the polymer strip at the operating temperature. The gas pressure associated with each equilibrium point was measured with a digital pressure gauge (model PM) from Heise (Stratford, CT) with a full scale reading of 300 psig and an accuracy of 0.025% of full scale. A refrigerated bath circulator (model RTE 740) from Thermo Electron Co. (Newington, NH), operating with a 50 wt % ethylene glycol solution as cooling fluid, provided for temperature control.

2.3. Sorption Measurements. Gas solubility in the polymer was determined on the basis of the barometric pressure–decay method utilizing a dual-volume, dual-transducer apparatus.³⁴ It basically consists of two interconnected chambers of known volume immersed in a temperature-controlled bath. A known amount of XLPEO film was placed inside the sample chamber and degassed at least overnight before beginning an experiment. A known amount of gas was introduced into the sample chamber, whose pressure then decreased as sorption occurred. Once equilibrium was achieved, which could take from 90 min to 4 days depending on the operating temperature and on the gas under study, more gas was introduced into the sample chamber to determine solubility as a function of pressure. Detailed descriptions of a general setup and procedure for this experiment can be found elsewhere.^{35,36}

Pressure in each chamber was measured by a Super TJE transducer from Honeywell Sensotec (Columbus, OH) with a full scale reading of 500 psia and an accuracy of 0.05% of full scale. The cell volumes, (17.81 ± 0.09) and $(13.17 \pm 0.07) \text{ cm}^3$, were determined according to the method proposed by Burnett.³⁷ A refrigerated bath circulator (Neslab RTE 140), operating with an aqueous solution containing 50 wt % methanol as cooling fluid, provided temperature control. The changes in the gas phase volume of the polymer-containing cell due to sorptive and thermal dilation of the polymer sample were taken into account in the mass balances using data from dilation measurements. Blank runs without the polymer performed in our laboratory²⁶ have proven that gas adsorption on the walls of the sorption cells makes a negligible contribution to the observed sorption over the pressure and temperature operating ranges considered in this study.

The pressure decay method relies on an equation of state to transform the pressure reduction observations into a sorption isotherm via mass balances.^{35,36} In this work, the virial equation of state truncated to three terms³⁸ was adopted. Taking into account that the calculated concentration of gas in the polymer is rather

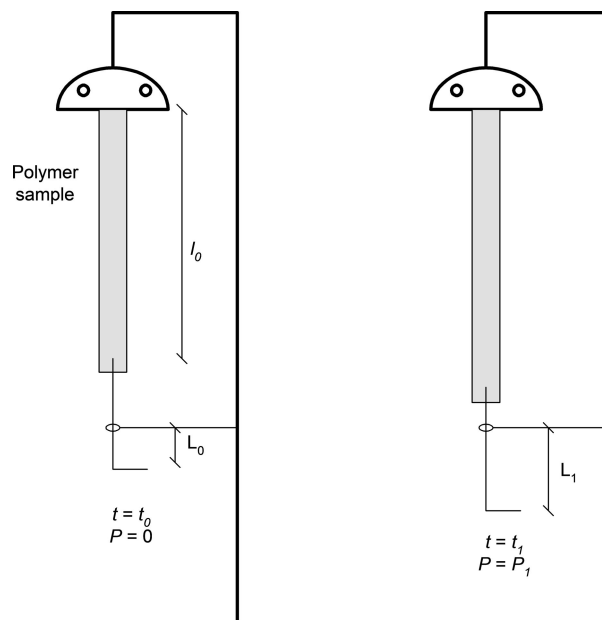


Figure 1. Measuring principle for dilation experiments.

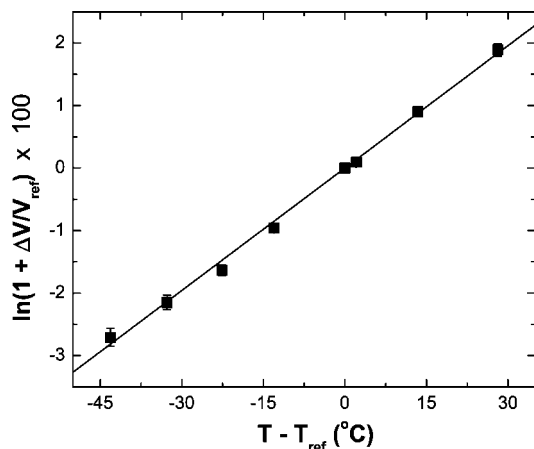


Figure 2. Thermal expansion of XLPEO under vacuum. $T_{\text{ref}} = 23^\circ\text{C}$.

sensitive to small errors in the gas compressibility factor,³⁹ special attention was given to the choice of virial coefficients reported in the literature.⁴⁰ Density predictions associated with different sets of virial coefficients were compared to experimental data for the temperature and pressure range covered in this work, and the coefficients associated with the smallest mean absolute deviation for the whole data set were chosen. In the case of carbon dioxide, a total of 130 density data^{41,42} was considered, and the mean prediction error was 0.012%, whereas, for ethane, 112 data^{42,43} were included in the comparison, and the mean prediction error was 0.045%. Details regarding the gas density calculation are given in the Appendix.

3. Results and Discussion

3.1. Polymer Dilation. Before the swelling effect due to polymer dilation could be investigated, it was necessary to determine the thermal expansion coefficient (α) of XLPEO prepared from pure PEGDA. This parameter is defined as follows:⁴⁴

$$\alpha = \frac{1}{V} \left(\frac{\partial V}{\partial T} \right)_P \quad (2)$$

Using the known volume, V_{ref} , at a given reference temperature, T_{ref} , and assuming α to be independent of temperature, eq 2 can be integrated to give

$$V(T) = V_{\text{ref}} \exp[\alpha(T - T_{\text{ref}})] \quad (3)$$

In terms of volume change, $\Delta V = V(T) - V_{\text{ref}}$, eq 3 can be rearranged as follows:

$$\ln \left(1 + \frac{\Delta V}{V_{\text{ref}}} \right) = \alpha(T - T_{\text{ref}}) \quad (4)$$

which can be used to calculate α as the slope of a least-squares fit (through the origin) of a volume-versus-temperature data set.

Thus, with the aid of the dilation apparatus, changes in the sample volume as a function of operating temperature were measured under vacuum. Any temperature at which the polymer density is known can be utilized as a reference, and, in this work, $T_{\text{ref}} = 23.0^\circ\text{C}$. The results, expressed in accordance with eq 4, are plotted in Figure 2. The line shown in this figure represents the least-squares fit of the data, from which $\alpha = (6.53 \pm 0.14) \times 10^{-4} \text{ K}^{-1}$. This value is in very good agreement with the one reported by Van Krevelen⁴⁵ for poly(ethylene oxide), $\alpha = (6.2\text{--}6.6) \times 10^{-4} \text{ K}^{-1}$.

Once the thermal expansion coefficient was determined, the relative increase in the volume of the polymer sample due to gas sorption was measured at five different temperatures. The results are presented in Figure 3 as a function of gas fugacity,

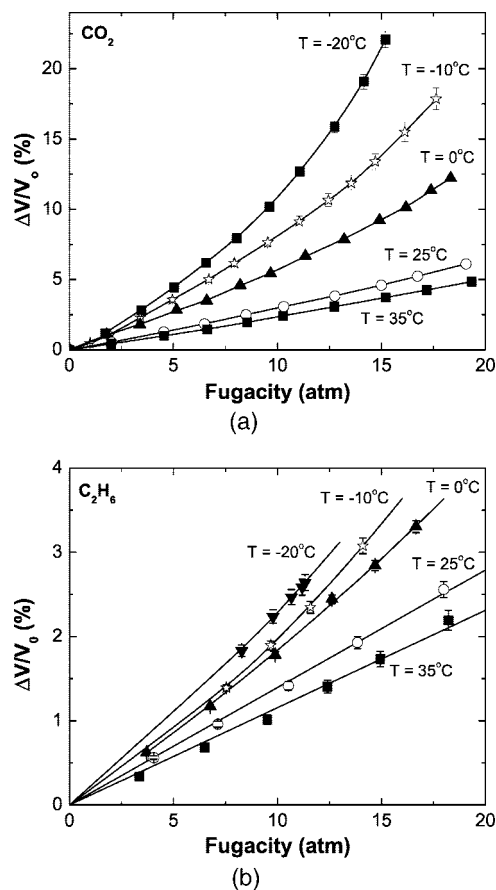


Figure 3. Sorptive dilation of XLPEO as a function of gas fugacity for carbon dioxide (a) and ethane (b) at different operating temperatures. The lines are drawn to guide the eye.

whose value was computed with the virial equation of state, as described in the Appendix. For each temperature, the penetrant-free volume, V_0 , was obtained utilizing eq 3.

For both gases, the volume of the polymer always increases with increasing gas fugacity, an effect which becomes more pronounced as temperature decreases. Both trends are a direct consequence of changes in the amount of gas sorbed by the polymer at a given operating condition, as will be shown below. In the case of CO_2 , due to its high affinity for the polymer, the dilation isotherms in Figure 3 are always convex to the fugacity axis, and the volume increase can be rather significant, especially at lower temperatures, for which dilation values greater than 20% can be observed. Ethane, on the other hand, has a much less pronounced effect, and within the investigated range of operating parameters, the change in the volume of the polymer did not surpass 4%. The polymer volume increases linearly at the two highest temperatures in Figure 3b, while at 0°C a slight curvature in the dilation isotherm is perceived, whose presence becomes more evident as temperature is further reduced.

3.2. Gas Sorption. Sorption isotherms for carbon dioxide and ethane in XLPEO at the different operating temperatures considered in this work are presented in Figure 4. The results are expressed as the concentration (C) of gas sorbed in the polymer per unit volume of the corresponding penetrant-free polymer at the operating temperature (given by eq 3).

First, the equilibrium concentrations of CO_2 in the polymer are rather high, especially relative to the ethane uptake values. For all temperatures, a nonlinear increase in the equilibrium gas concentration with the gas fugacity is observed in Figure 4a. At a given fugacity, the sorbed CO_2 concentration increases considerably as operating temperature is reduced. Both trends

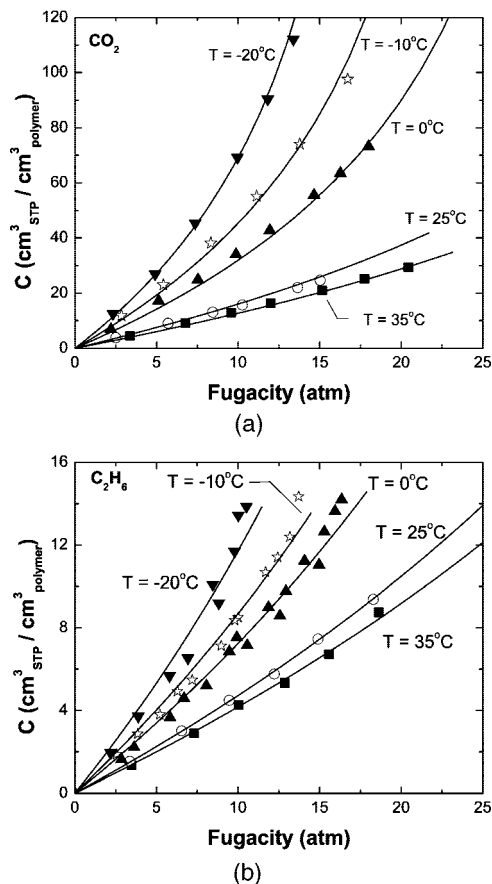


Figure 4. Sorption isotherms for carbon dioxide (a) and ethane (b) in XLPEO as a function of gas fugacity at five different temperatures. The lines are the prediction of the Flory–Huggins model with the parameters fitted in this work.

are typical when highly soluble penetrants sorb into rubbery polymers.^{32,46} Equilibrium concentrations are approximately 1 order of magnitude lower for ethane, as this gas, in contrast to carbon dioxide, has no specific interactions with the ether groups in the polymeric chain. The isotherms are practically linear at the two highest temperatures, but a slight curvature becomes evident in Figure 4b as the temperature decreases and gas condensability increases. A comparison between Figures 3 and 4 shows that, as expected, higher volume changes are associated with the dissolution of larger amounts of gas in the polymer. For this reason, the dilation and sorption isotherms bear a strong qualitative resemblance to each other.

To model the sorption isotherms, the traditional Flory–Huggins equation was adopted:^{46,47}

$$\ln \frac{f}{f_{\text{sat}}} = \ln \phi + (1 - \phi) + \chi(1 - \phi)^2 \quad (5)$$

where f is the fugacity of the gas in equilibrium with the polymer, f_{sat} is the saturation fugacity of the gas at the operating temperature, χ is the Flory–Huggins interaction parameter, which has to be fitted for each polymer–penetrant system, and ϕ is the volume fraction of the penetrant in the polymer. The values of C and ϕ can be related to each other with the aid of the partial molar volume of the gas in the polymer (\bar{V}):

$$\phi = \frac{C\bar{V}}{22\,414 + C\bar{V}} \quad (6)$$

Partial molar volumes for each gas in XLPEO as a function of temperature were obtained in this work by combining results from gas sorption and dilation measurements, as detailed in

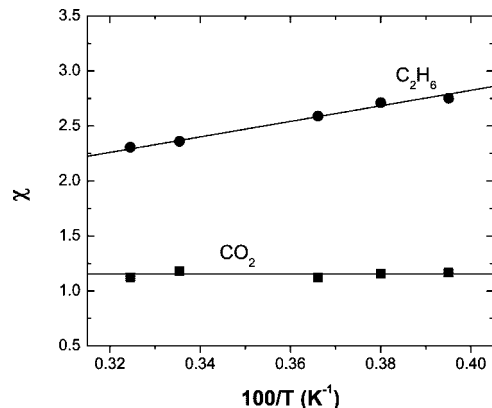


Figure 5. Flory–Huggins interaction parameters fitted in this work for carbon dioxide and ethane in XLPEO as a function of temperature.

section 3.3. At all temperatures, the gas saturation pressure, required for the calculation of f_{sat} , was estimated using the expressions given by Liley et al.⁴⁴ For each isotherm, the parameter χ was fitted by the maximum likelihood method⁴⁸ with an objective function in terms of C utilizing the software ESTIMA.⁴⁹ The computed values for χ are plotted in Figure 5. The fitted isotherms, shown as continuous lines in Figure 4, are in good agreement with the experimental results.

In the case of ethane, the inverse dependence of χ on temperature anticipated by the Flory–Huggins theory⁴⁷ is observed, and the individual values are always greater than 2.0 within the temperature range considered, which is an indication of low solubility of gas in the polymer.⁴⁶ A least-squares linear fit of the data in Figure 5 gives a slope equal to (706 ± 3) K (with $R^2 = 0.9856$), which, based on the definition⁴⁷ of χ ($\chi \equiv W_{1,2}/RT$), corresponds to an interaction energy, $W_{1,2}$, of (5.87 ± 0.02) kJ/mol between XLPEO and ethane. This positive value of $W_{1,2}$ indicates that the dissolution of ethane in XLPEO, according to the hypotheses of the Flory–Huggins theory, would be an endothermic process.

With regard to carbon dioxide, the values fitted for each temperature seemed to randomly oscillate around a mean value. Therefore, a new fitting was performed, considering a single χ for all isotherms, which led to $\chi = (1.1564 \pm 0.0063)$, the value that is plotted in Figure 5 as a constant line. All fitted isotherms shown in Figure 4a were calculated using this constant value. Similar behavior was recently observed by Raharjo et al.³² for the sorption of *n*-butane in poly(dimethyl siloxane) over an even wider temperature range (-20 to 50 °C). Referring to the definition of χ , a temperature-independent value implies a linear dependence of $W_{1,2}$ on T . Thus, within the framework of the Flory–Huggins theory, in the case of the CO_2 –XLPEO system, because χ is positive, the dissolution of the gas would become less endothermic at lower temperatures, or, in other words, the gas–polymer interaction would increase with decreasing temperature.

In a previous study with the same system and temperature range considered here, Lin and Freeman²⁶ reported that an empirical dependence of χ on temperature and penetrant volume fraction was necessary to properly fit the sorption isotherms. The causes for this apparent contradiction are believed to be 2-fold. First, because no information on the sorptive or thermal dilation of XLPEO was previously available, both effects were not taken into account in the measurement of the sorption isotherms. Second, the partial molar volume of the gases was assumed to be independent of temperature, and literature values related to other rubbery polymers were employed. The validity of this latter assumption will be addressed in the next section. To assess exactly how significant the effect of polymer dilation

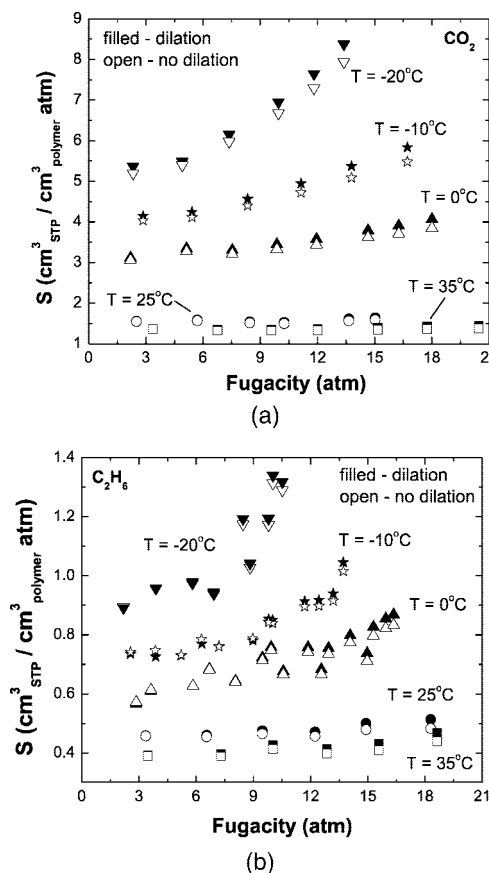


Figure 6. Gas solubility for carbon dioxide (a) and ethane (b) in XLPEO as a function of fugacity at different temperatures obtained from the same pressure–decay data but with and without considering changes in the volume of the polymer sample due to thermal and sorptive dilation.

can be in the measurement of sorption isotherms by the pressure–decay method, the same raw data used to calculate the isotherms presented in Figure 4 were also processed to determine the corresponding isotherms when polymer dilation is neglected. The two sets of isotherms for each gas are compared in Figure 6 in terms of the gas solubility, S , defined as:

$$S = \frac{C}{f} \quad (7)$$

It is clear from Figure 6 that the neglect of volume changes in the polymer sample due to gas sorption and thermal expansion can lead to different sorption isotherms for the same set of pressure–decay data. For carbon dioxide, because sorptive dilation is much more significant than thermal expansion, their neglect always results in an underestimation of the gas solubility, whose extent grows with gas fugacity due to the increasing sorptive dilation at higher fugacity. This underestimation varied from 0.65% ($f = 3.36$ atm at 35 °C) to 6.1% ($f = 16.7$ atm at −10 °C). As seen in Figure 6b, the effects may be significant even for ethane, whose sorption causes much less change in the volume of the polymer than that of CO₂. In fact, as sorptive dilation and thermal expansion are of the same order of magnitude in this case, some fortuitous error compensations can occur. At the two highest temperatures, considering that the polymer density was measured at $T_{\text{ref}} = 23$ °C, the volume changes due to sorption and thermal effects have the same sign, and the trend is similar to the one observed for CO₂, that is, an underestimated solubility. Even though the absolute differences in the values of S due to neglecting dilation are smaller for

ethane, the relative underestimation is actually higher, varying from 0.22% ($f = 3.35$ atm at 25 °C) to 6.0% ($f = 18.6$ atm at 35 °C). This probably stems from the fact that the pressure drop in the sample chamber due to gas sorption is much lower for ethane and, therefore, the computed amount of sorbed gas is more sensitive to errors in the volume occupied by the gas in the sample chamber. Focusing now on $T < T_{\text{ref}}$, and Figure 6b, ethane solubility is, in fact, overestimated at low fugacities, when the decrease in the polymer volume due to the temperature reduction is greater than the volume increase due to gas sorption. As the gas pressure, and consequently its fugacity, is progressively increased, the sorptive dilation of the polymer becomes more pronounced, whereas the thermal effect remains constant. The net effect is a lower error in the estimation of the gas volume in the polymer-containing chamber, and the two solubilities thus become closer. At the point where these two effects counterbalance, the same solubility value is obtained. From this point on, the polymer volume is always underestimated when dilation is neglected, leading to an underestimation of gas solubility.

Although the data in Figure 6 are plotted as a function of gas fugacity in equilibrium with the polymer, the absolute error in gas solubility depends not only on this variable, but also on how it was reached during the experiment. This fact is evident, for instance, in the data set for ethane at $T = -10$ °C and $f < 8$, which comes from two different experiments. The absolute overestimation of gas solubility varies from point to point, even though it gets closer to zero in each set of data as f increases. At the beginning of each run, because the sample chamber is under vacuum, the error in the polymer volume only affects the final amount of gas in this chamber, whereas, once the sequential increase in pressure inside the sample chamber is started, both initial and final amounts of gas are subjected to errors in the polymer volume due to neglecting the dilation effect. The absolute value of these errors will depend on the magnitude of the pressure increase, which explains why the final error in S when dilation is neglected will be a function of both the equilibrium gas fugacity and the experimental procedure adopted to reach it.

With regard to the effect of temperature on gas solubility, in the limit of infinite dilution, when the sorbed gas concentration is very low, the Flory–Huggins model reduces to Henry's law, $C = S_{\infty}f$, where S_{∞} is the infinite dilution solubility of the gas in the polymer:¹⁸

$$S_{\infty} = \frac{22\,414}{f_{\text{sat}} \bar{V}} \exp[-(1 + \chi)] \quad (8)$$

Using eq 8 and the values of χ and \bar{V} obtained in this work, the infinite dilution solubility of carbon dioxide and ethane in XLPEO was computed at the different operating temperatures considered. The results are portrayed in Figure 7, and the lines correspond to a least-squares fit of the data to the van't Hoff equation for gas dissolution, traditionally employed in the literature to describe the temperature dependence of S_{∞} .⁴⁶

$$S_{\infty} = S_0 \exp\left(-\frac{\Delta H_s}{RT}\right) \quad (9)$$

Both gases show a positive slope in Figure 7, and, therefore, according to eq 9, their enthalpy of sorption, ΔH_s , is negative for XLPEO, indicating an exothermic process. The values of ΔH_s for both gases are compared in Table 1 with literature data^{50–58} related to other polymers. In the case of ethane, all polymers except TFE/BDD87 exhibit a similar value for ΔH_s . For carbon dioxide, XLPEO exhibits the lowest ΔH_s (i.e., most exothermic) value among the polymers, which could be misinterpreted as evidence for the strong interaction between these two species. However, as highlighted in Table 1, each

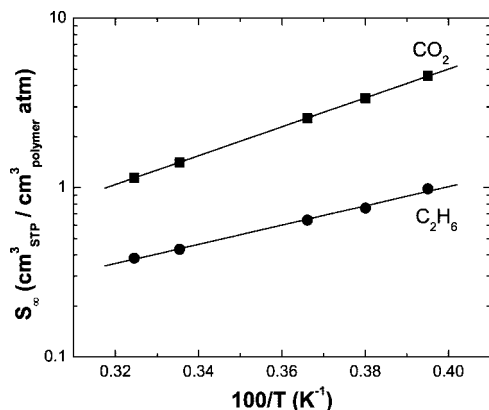


Figure 7. Infinite dilution solubility of carbon dioxide and ethane in XLPEO as a function of temperature. The lines correspond to least-squares fits to eq 9.

ΔH_S value is associated with a different temperature range, and to draw a comparison in a more appropriate basis, we shall refer to the usual analysis of gas dissolution into a polymer as a two-step thermodynamic process:⁴⁶ (i) condensation of the gas to a liquid-like state (or, in the case of supercritical gases, to a condensed density consistent with that of the polymer), and (ii) mixing of condensed gas with polymer segments. The enthalpy of sorption can now be decomposed into two terms, the enthalpy of condensation (ΔH_{cond}), a temperature-dependent property of the gas, and the enthalpy of mixing (ΔH_{mix}), which is a function of the polymer–gas pair:

$$\Delta H_S = \Delta H_{\text{cond}} + \Delta H_{\text{mix}} \quad (10)$$

On the basis of the concept of the mean value of a function over a given interval of its domain, an average enthalpy of condensation for a temperature range $T_1 \leq T \leq T_2$ can be defined as follows:

$$\overline{\Delta H_{\text{cond}}} = \frac{1}{T_2 - T_1} \int_{T_1}^{T_2} \Delta H_{\text{cond}}(T) dT \quad (11)$$

Using the function $\Delta H_{\text{cond}}(T)$ presented by Liley et al.,⁴⁴ eq 11 was applied to each gas and temperature range considered in Table 1, and the obtained $\overline{\Delta H_{\text{cond}}}$ was substituted into eq 10 to yield the corresponding ΔH_{mix} . All studies covered temperatures higher than the critical temperature of the gases, T_c , but because ΔH_{cond} is not defined for $T > T_c$, all calculations were made using $T_2 = T_c$. The final results are listed in Table 1. In particular, for EP, because the lowest temperature investigated by Tsuboi et al.⁵⁸ was already higher than T_c , the value of $\overline{\Delta H_{\text{cond}}}$ could not be evaluated.

Once the differences in temperature ranges are properly addressed, the high absolute value of ΔH_S obtained for CO₂ in XLPEO is actually a result of the large contribution of ΔH_{cond} to ΔH_S . For both carbon dioxide and ethane, the largest absolute value of ΔH_{mix} is associated with the glassy polymer TFE/BDD87. Because of the presence of nonequilibrium excess free volume (NEFV), glassy polymers normally require a less endothermic contribution to accommodate penetrant molecules in the polymer matrix than rubbers, for which a molecular-scale gap must be created in the polymer matrix to enable gas sorption.⁴⁶ This aspect is especially important in the case of TFE/BDD87, whose NEFV at 25 °C is 48.1 mm³/g.⁵⁹ For this particular amorphous fluoropolymer, the value of fractional free volume, 0.32, is among the highest ever reported for a dense polymer and is similar to that of poly(1-trimethylsilyl-1-propyne), the most permeable polymer known.⁵⁶ Focusing on carbon dioxide, the two methacrylates, PBMA and PEMA, follow TFE/BDD87 in the increasing order of ΔH_{mix} . For these

polymers, the value of ΔH_S listed in Table 1 was computed mostly (but not exclusively) with data related to the glassy state. Even though the NEFV is not as high as that of TFE/BDD87, the carbonyl groups in methacrylates are known to exhibit specific interactions with CO₂, most probably of a Lewis acid–base nature.⁶⁰ The higher absolute value observed for PBMA as compared to PEMA can be rationalized in terms of a larger NEFV due to the substitution of a hydrogen by a bulky phenyl group in the polymer chain. All other polymers in Table 1 are rubbery for $T \leq T_c$ and show a higher ΔH_{mix} than does XLPEO. Thus, the favorable interaction between CO₂ and the ether groups in XLPEO leads to the most exothermic mixing among the rubbery polymers included in Table 1. The comparison with LDPE is particularly interesting, because the lack of the ether group in the polymer chain is a key difference in relation to XLPEO. The absolute value of ΔH_{mix} is more than twice as large in XLPEO, in good agreement with the notion that there is a strong interaction between carbon dioxide and the ether groups in the polymer chain. In the case of ethane, no specific interaction with ether groups is expected, and, accordingly, the enthalpy of mixing obtained in this work for XLPEO agrees, within the experimental error, with the one reported by Michaels and Bixler⁵⁰ for PE.

Contrary to the predictions of the Flory–Huggins theory, ΔH_{mix} values in XLPEO, as well as in the other rubbery polymers included in Table 1, are negative, a fact that has already been reported in the literature for other systems.²⁶ Despite its ability to represent the experimental sorption isotherms, the Flory–Huggins model includes the assumption that penetrant molecules and segments of the polymer chain (each segment being of the same size as the penetrant and the chain comprising N connected segments) can be moved in space without any changes in the interactions of neighboring particles,⁴⁷ which is not strictly true, especially in the case of carbon dioxide sorption in XLPEO, for which a strong, specific gas–polymer interaction is known to take place.

3.3. Partial Molar Volumes. If sorption and dilation data are available for a given polymer–penetrant pair, these can be combined to estimate the partial molar volume (PMV) of the gas in the polymer,⁵⁴ \bar{V} :

$$\bar{V} = 22\,414 \left\{ \frac{d}{dC} \left[\left(1 + \frac{\Delta V}{V_0} \right) (1 + \beta P) \right] - \beta P \frac{d}{dC} \left(1 + \frac{\Delta V}{V_0} \right) \right\} \quad (12)$$

where β is the isothermal compressibility of the penetrant-free polymer ($\beta = -(\partial \ln V / \partial P)_{P,T}$). For high-solubility gases, the terms involving β in eq 12 are usually small and can be neglected in the calculation of \bar{V} up to moderate pressures, whereas, in the case of low-solubility penetrants, all terms may be significant. Whenever polymer compression is not significant, the previous equation can be simplified to:

$$\bar{V} = 22\,414 \frac{d}{dC} \left(1 + \frac{\Delta V}{V_0} \right) \quad (13)$$

To the best of our knowledge, no experimental value for the compressibility of XLPEO prepared from PEGDA is available in the literature, and in an attempt to measure at least the order of magnitude of β for this material, a dilation experiment was performed at 35 °C with helium, whose sorption in rubbery polymers is rather low due to its low condensability. Even at an operating pressure of 33.4 atm, which is 57% higher than the maximum pressure used in the experiments with carbon dioxide and ethane, no change in the length of the polymer strip was detected. Lower pressures were also tested, and once again neither a positive nor a negative change in length was observed, so the hypothesis of a sorptive dilation that would exactly

Table 1. Enthalpies of Sorption, Condensation, and Mixing at Infinite Dilution for the Sorption of Carbon Dioxide and Ethane in Polyethylene (PE), Low-Density Polyethylene (LDPE), Poly(ethyl methacrylate) (PEMA), Polybutadiene (PB), Poly(ethylene-co-vinyl acetate) (PE-co-VA), Poly(benzyl methacrylate) (PBMA), Poly(2,2-bis(trifluoromethyl)-4,5-difluoro-1,3-dioxole-co-tetrafluoroethylene) (TFE/BDD87), Poly(dimethyl siloxane) (PDMS), Ethylene-Propylene Copolymer (EP), and Cross-linked Poly(ethylene oxide) (XLPEO)

polymer	ΔH_s (kJ/mol)	T range (°C)	ΔH_{cond} (kJ/mol)	ΔH_{mix} (kJ/mol)	reference
CO ₂ in Rubbery Polymers					
PDMS	-10.8	-30 to 55	-9.51	-1.29	Kamiya et al. ⁵⁷
PE-co-VA	-7.95	10–40	-6.19	-1.76	Kamiya et al. ⁵⁴
PB	-8.37	15–80	-5.56	-2.81	Kamiya et al. ⁵²
LDPE	-7.28	25–55	-3.80	-3.48	Hirose et al. ⁵¹
XLPEO	-16.32 ± 0.06	-20 to 35	-8.85	-7.47 ± 0.06	this work
CO ₂ in Glassy Polymers					
PEMA	-14.6	15–85	-5.56	-9.04	Kamiya et al. ⁵³
PBMA	-13.8	25–75	-3.80	-10.0	Wang et al. ⁵⁵
TFE/BDD87	-14.8	25–45	-3.80	-11.0	Merkel et al. ⁵⁶
C ₂ H ₆ in Rubbery Polymers					
XLPEO	-10.9 ± 0.4	-20 to 35	-7.93	-3.0 ± 0.4	this work
PE	-9.63	5–55	-6.18	-3.45	Michaels and Bixler ⁵⁰
EP	-11.0	56–62			Tsuboi et al. ⁵⁸
C ₂ H ₆ in a Glassy Polymer					
TFE/BDD87	-14.2	25–45	-3.70	-10.5	Merkel et al. ⁵⁶

counterbalance the polymer compression is not correct. Thus, in all cases, the actual length reduction due to the compression of the polymer was smaller than the highest resolution of our setup, which was 13 μm . Therefore, according to eq 1, $\Delta V/V_0 < 5.25 \times 10^{-4}$ at 33.4 atm, which implies that $\beta < 1.57 \times 10^{-5} \text{ atm}^{-1}$ for XLPEO. The order of magnitude of this upper estimate of β compares very favorably with the experimental value of $1.78 \times 10^{-5} \text{ atm}^{-1}$ given by Van Krevelen⁴⁵ for poly(ethylene oxide).

Using the sorption and dilation data for carbon dioxide and ethane at 25 °C, PMVs calculated on the basis of eq 13 were compared to those obtained from eq 12 with $\beta = 1.57 \times 10^{-5} \text{ atm}^{-1}$. The differences in the PMVs were equal to 0.5 and 1.4% for carbon dioxide and ethane, respectively, mainly due to the contribution of the first term involving β in eq 13. Considering that these differences are still within the experimental errors associated with the PMVs for each gas together with the fact that they are related to an overestimated value for β , all PMVs in this work were computed neglecting polymer compression, that is, utilizing eq 13. The final results are shown as a function of temperature in Figure 8. In analogy with the framework

adopted for gases dissolved in liquids, the effect of temperature on the PMV was represented in terms of a thermal expansion coefficient for the gas dissolved in the polymer, α_i^* , whose definition is exactly the same as that used for pure species (eq 2), just replacing V by \bar{V} :

$$\bar{V}_i(T) = \bar{V}_{i,\text{ref}} \exp[\alpha_i^*(T - T_{\text{ref}})] \quad (14)$$

Equation 14 was fitted to our data, using $T_{\text{ref}} = 25$ °C and the corresponding experimental value of \bar{V}_i as $\bar{V}_{i,\text{ref}}$. The resulting values of α_i^* are given in Table 2, and the corresponding predictions are shown as continuous lines in Figure 8. In view of the slight scatter in the data set, eq 14 provides a good representation of PMVs and their dependence upon temperature in this system. For comparison, upon applying eq 14 to volumetric data⁴³ of liquid ethane at 4.5 and 5.2 MPa and $260 \leq T \leq 300$ K, α values of 9.19×10^{-3} and $7.67 \times 10^{-3} \text{ K}^{-1}$, respectively, are obtained (the data actually showed a dependency of α upon temperature, but both fits gave $R^2 > 0.9$). With regard to carbon dioxide, the fitting of eq 14 to volumetric data⁴⁴ for saturated liquid CO₂ between 245 and 280 K gives $\alpha = 5.67 \times 10^{-3} \text{ K}^{-1}$. Strictly speaking, this value is not the thermal expansion defined by eq 2, because the liquid is saturated, and pressure, therefore, varies with temperature, but the data were fitted with $R^2 > 0.98$. These values are close to those obtained for α_i^* . Although the pressure and temperature ranges are not exactly the same for the values related to pure liquids and gases dissolved in polymers, the latter are smaller than the former for both penetrants, a fact that can actually be physically rationalized, as it shall be later demonstrated in this section.

Excluding the pioneering work of Ham et al.,⁶¹ dilation data for polymers started to appear in the literature in the 1980s, and since then, it has been reported that PMVs of gases dissolved in rubbery polymers and in liquids are similar, without any correlation whatsoever between the polymer structure and the actual PMV of the gas. The standard procedure^{51,62} is to compare the value in the polymer with an average for different organic solvents, as well as with values for other polymers, to check whether these are similar. Differences among rubbery polymers are believed to be due to data scatter and, to the best of our knowledge, have never been systematically discussed. In the case of carbon dioxide, data for different rubbery polymers have even been used to fit an empirical equation for the PMV as a function of temperature:⁶³

$$\bar{V}_{\text{CO}_2} = 44.0[1 + (2.1 \times 10^{-3})(T - 298)] \quad (15)$$

where \bar{V}_{CO_2} is given in cm^3/mol and T in K.

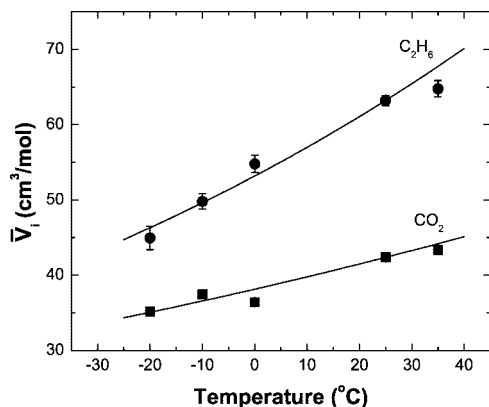


Figure 8. Partial molar volumes of carbon dioxide and ethane in XLPEO as a function of temperature. The lines correspond to the prediction of eq 14 with the parameters given in Table 2.

Table 2. Parameters for Calculation of Partial Molar Volumes in XLPEO Using Eq 14

gas	$\bar{V}_{i,\text{ref}}$ (cm^3/mol)	$\alpha_i^* \times 10^3$ (K^{-1})
CO ₂	42.4 ± 0.1	4.2 ± 0.4
C ₂ H ₆	63.2 ± 0.7	6.9 ± 0.5

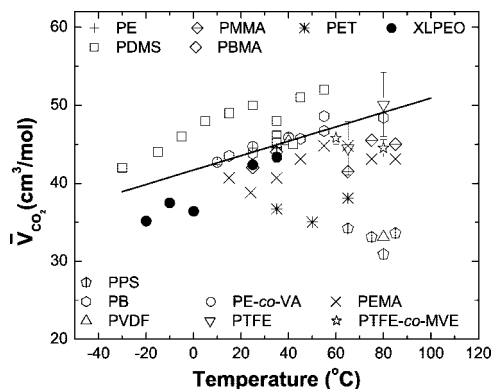


Figure 9. Partial molar volumes of carbon dioxide in 13 different rubbery polymers as a function of temperature: polybutadiene (PB),⁵² poly(ethylene-co-vinyl acetate) (PE-co-VA),⁵⁴ poly(vinylidene fluoride) (PVDF),^{68,70} low-density polyethylene (PE),⁵¹ poly(ethyl methacrylate)⁵³ (PEMA), poly(dimethyl siloxane) (PDMS),^{57,62,66,67,69} poly(tetrafluoroethylene-co-perfluoromethylvinylether) (PTFE-co-MVE),⁷⁰ poly(tetrafluoroethylene) (PTFE),⁷⁰ poly(*p*-phenylene sulfide) (PPS),⁶⁵ poly(ethylene terephthalate) (PET),⁶⁴ poly(benzyl methacrylate) (PBMA),⁵⁵ poly(methyl methacrylate) (PMMA),⁶³ and cross-linked poly(ethylene oxide) (XLPEO, this work). The line corresponds to the prediction of eq 15.

Following this standard data treatment procedure, we compare our PMVs for CO₂ in XLPEO with available literature data for 12 rubbery polymers^{51–55,57,62–70} in Figure 9. The prediction of eq 15 is also included in the referred figure as a continuous line. For the cases when the operating temperature was lower than the glass transition temperature of the polymer (T_g), the data were obtained after enough CO₂ had been sorbed to bring about an isothermal glass transition. An increasing trend for PMV as a function of temperature is confirmed in this figure, but at a given temperature, values from different polymers can vary significantly. Some data do agree with the predictions of eq 15, but our values for XLPEO are somewhat lower than such predictions, and the difference seems to increase as temperature decreases.

The sorption data discussed in section 3.2 show a strong affinity of XLPEO for carbon dioxide, with an unusually high enthalpy of mixing as compared to other rubbery polymers. Furthermore, XLPEO has a polar structure, whereas most rubbery polymers from previous studies were nonpolar. Taking these aspects into account, it seemed unlikely that our lower PMVs were merely a result of data scatter, and we decided to investigate whether the differences among polymers in Figure 9 could be somehow rationalized at a molecular level.

To do so, a quantitative variable directly related to the molecular structure of the polymer was necessary to enable the comparison of PMVs in different materials at a given temperature. The solubility parameter, δ , which describes the attractive strength between molecules of a given substance and is, therefore, directly connected to the polarity of its molecules, seemed a plausible choice. Because gases dissolved in liquids and rubbery polymers are recognized to be in a similar thermodynamic state, and a larger amount of PMV data is available in the case of liquids, the idea was first tested for liquids. Thus, PMVs for carbon dioxide and ethane at 25 °C in liquids^{71–83} are plotted in Figure 10 as a function of the solubility parameter of the solvent. Solubility parameters were taken from Grulke⁸⁴ for all solvents except tetradecane ($\delta = 16.3$ MPa^{1/2}) and methyl cyanoacetate ($\delta = 28.3$ MPa^{1/2}), for which δ was computed on the basis of its definition.⁸⁴

Rather than a random pattern, a well-defined trend is observed for both gases, a decrease in PMV as δ increases and, consequently, as the solvent becomes more polar. The difference

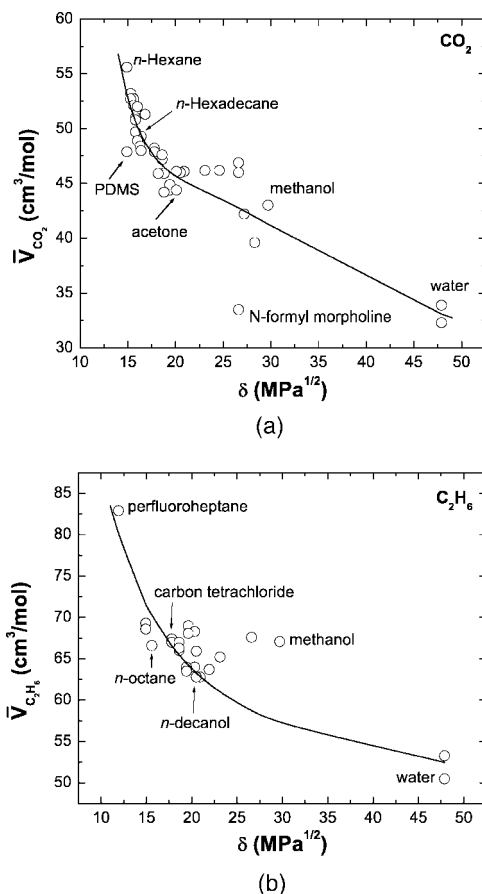


Figure 10. Infinite-dilution partial molar volumes of carbon dioxide (a) and ethane (b) in different liquids at 25 °C as a function of the solubility parameter of the solvent. Data for CO₂ were taken from Horiuti⁷¹ (acetone, methyl acetate, benzene, chlorobenzene, carbon tetrachloride), Hildebrand and Scott⁷² (methanol), Weiss⁷⁷ (water), Moore et al.⁷⁸ (water), Kamiya et al.⁸⁰ (PDMS), Xu et al.⁸¹ (propylene carbonate, methyl cyanoacetate, *n*-formyl morpholine), Cibulka and Heintz⁸² (*n*-hexane, *n*-heptane, *n*-octane, *n*-decane, *n*-hexadecane, ethanol, 1-propanol, 1-butanol, 1-octanol, 1-decanol), and Ashcroft and Isa⁸³ (*n*-heptane, *n*-octane, *n*-nonane, *n*-decane, *n*-dodecane, *n*-tetradecane, *n*-hexadecane, cyclohexane, methylcyclohexane, toluene). Data for ethane were taken from Horiuti⁷¹ (acetone, chlorobenzene, methyl acetate), Gjaldbæk and Hildebrand⁷³ (perfluoroheptane, carbon disulfide, carbon tetrachloride, *n*-hexane, benzene), Hildebrand and Scott⁷² (acetone, methyl acetate, carbon tetrachloride, benzene, chlorobenzene), Masterton⁷⁴ (water), Ng and Walkley⁷⁵ (*n*-hexane, benzene), Tiepel and Gubbins⁷⁶ (water), and Handa et al.⁷⁹ (*n*-octane, methanol, ethanol, 1-butanol, 1-hexanol, 1-octanol, 1-decanol). The lines are drawn to guide the eye.

in the PMV among solvents can be quite substantial. For instance, as one goes from *n*-hexane to benzene, the PMV of CO₂ decreases from 55.6 to 47.2 cm³, reaching a value of 39.6 cm³ in methyl cyanoacetate. In the case of ethane, the difference in its PMV in perfluoroheptane and water is about 30 cm³. Based on Figure 10, it is evident that the PMV of a gas dissolved in a liquid does depend on the chemical structure of the matrix into which the gas is dissolving. Consequently, comparing PMVs of gases in rubbery polymers with an average value over different organic liquids should be regarded as a crude approximation of the actual situation. In fact, correlations for the prediction of PMV as a function of the solubility parameter of the liquid,^{79,85} as well as a theoretical explanation⁸⁶ for the decreasing trend in Figure 10, have already been proposed. The explanation is given in terms of the internal pressure of the liquid solvent, π , which is directly linked to the solubility parameter ($\pi \approx \delta^2$). The solute is thought to behave like a gas being compressed to its liquid-like volume by the internal pressure

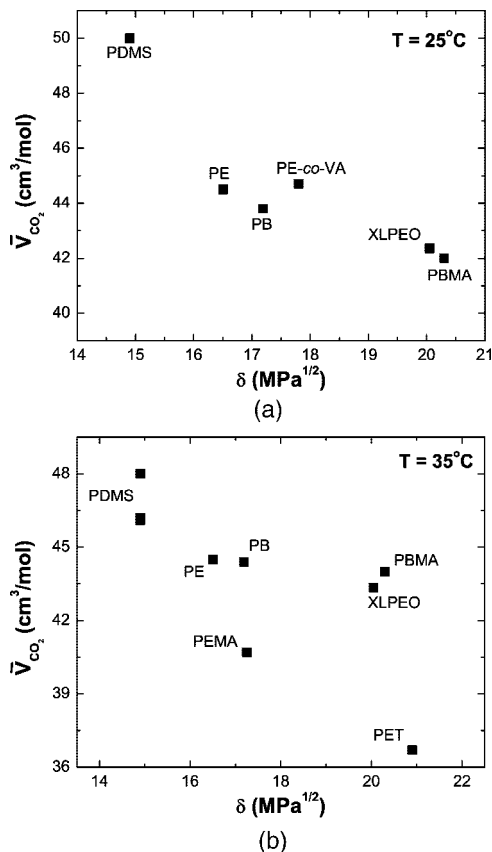


Figure 11. Partial molar volumes of carbon dioxide in rubbery polymers at 25 °C (a) and at 35 °C (b) as a function of the solubility parameter of the polymer, including low-density polyethylene (PE),⁵¹ polybutadiene (PB),⁵² poly(ethylene-co-vinyl acetate) (PE-co-VA),⁵⁴ poly(benzyl methacrylate) (PBMA),⁵⁵ poly(dimethyl siloxane) (PDMS),^{57,62,66,69} poly(ethyl methacrylate)⁵³ (PEMA), poly(ethylene terephthalate) (PET),⁶⁴ and cross-linked poly(ethylene oxide) (XLPEO, this work).

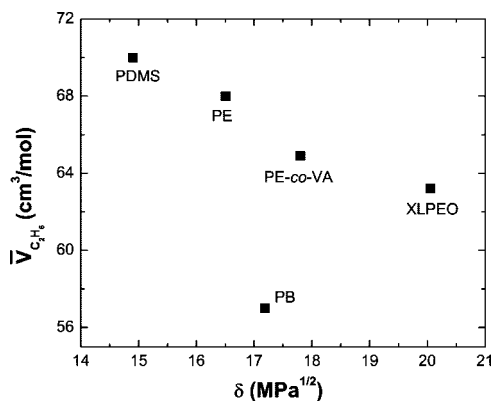


Figure 12. Partial molar volumes of ethane in rubbery polymers at 25 °C as a function of the solubility parameter of the polymer, including polybutadiene (PB),⁵² poly(ethylene-co-vinyl acetate) (PE-co-VA),⁸⁷ low-density polyethylene (PE),⁵⁷ poly(dimethyl siloxane) (PDMS),⁵⁷ and cross-linked poly(ethylene oxide) (XLPEO, this work).

of the solvent, with no further volume changes upon mixing the compressed solute with the solvent. Therefore, more polar liquids, whose attractive strength between molecules is larger, leading to higher π values, will exhibit lower PMVs for a given gas.

Encouraged by this promising outcome with liquids, we now compare, in Figures 11 and 12, PMVs in XLPEO for carbon dioxide and ethane with literature data for other rubbery polymers^{51–55,57,62,64,66,69,87} as a function of δ . Solubility

parameters for the polymers were taken from Van Krevelen,⁴⁵ Grulke,⁸⁴ and Charati and Stern,⁸⁸ using, for XLPEO, the value reported for poly(ethylene oxide). Strictly speaking, the solubility parameter itself is a function of temperature, and the values adopted in Figure 11b should have been corrected to 35 °C, but considering that such correction requires information that is not easily available for all polymers, and that the primary aim was to verify whether there would be any trend in the data set, δ values at 25 °C were employed in all plots.

Even though there are fewer data than in the case of liquids, the trend of decreasing PMV as solubility parameter increases is still evident for both gases. Thus, Figures 11 and 12 show a correlation between the chemical structure of the polymer and the PMV of the sorbed gas. Therefore, the differences observed in Figure 9 are not due simply to data scatter; they actually reflect differences at the molecular level in the interactions of CO₂ with these polymers. Furthermore, the use of a temperature- and polymer-independent PMV of a given gas to fit the Flory–Huggins model to its sorption isotherm in a rubbery polymer, as done for instance by Lin and Freeman¹⁸ in their previous study with XLPEO, is an approximation that can introduce errors into the evaluation of χ . Finally, it follows from Figure 11 that eq 15 is an oversimplification of the actual situation, because it is based on the assumption that the PMV of carbon dioxide does not depend on the chemical structure of the sorbing polymer.

The concept of internal pressure also applies to polymers, and the decreasing trend exhibited in Figures 11 and 12 can also be rationalized in terms of the same idea previously discussed for liquids. Additional factors intrinsic to macromolecules, such as degree of cross-linking and crystallinity levels, might play a role in the case of polymers, but more experimental data are necessary to address these issues.

This reasoning in terms of π can be utilized to explain two different aspects revealed in the present study concerning PMVs of gases in polymers. First, it explains why the thermal expansion coefficients of CO₂ and C₂H₆ dissolved in XLPEO are smaller than the values for pure liquids, because a decrease in α with increasing pressure is expected, and the internal pressure of this rubbery polymer is higher than that of liquid CO₂ and C₂H₆. A similar trend was reported,⁷⁴ for instance, in the case of benzene dissolved in water as compared to pure benzene. Second, this reasoning is in agreement with an increasing difference among polymers as the operating temperature decreases, because the attractive strength between molecules becomes stronger with decreasing temperatures, which would thus explain why, in Figure 9, our PMV data for CO₂ in XLPEO progressively deviate from the predictions of the equation proposed by Kamiya et al.⁶³ based on data from less polar rubbery polymers.

Having demonstrated that the chemical structure of both liquids and rubbery polymers influences the PMV of the dissolved gas, one could now ask whether the thermodynamic state of the dissolved gas is really the same in these two kinds of solvent, because such a conclusion has up to now been supported by comparisons of averages over different liquids and polymers, whose meaning is challenged by the results presented in Figures 10–12. Thus, in Figure 13, a comparison of the PMVs of CO₂ and C₂H₆ in liquids and rubbery polymers as a function of the solubility parameter is provided. All but one data point related to polymers lie very close to the corresponding data for liquids for a given solubility parameter, supporting, in a more formal way, the idea of a similar thermodynamic state of the dissolved gas in liquids and rubbery polymers. However, upon comparing the data sets related to the two gases, the PMV of carbon dioxide in the rubbery polymer seems to be slightly smaller than that in the liquid for a given δ , whereas, for ethane,

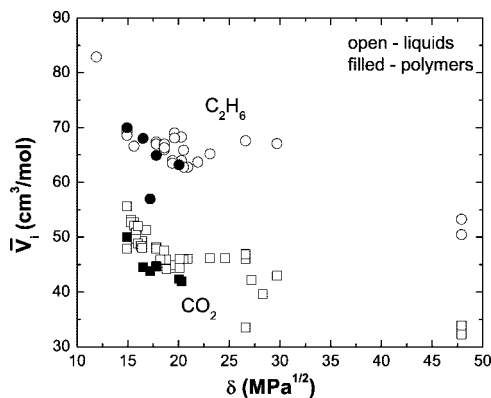


Figure 13. Comparison of partial molar volumes of carbon dioxide and ethane in liquids (open symbols) and rubbery polymers (filled symbols) at 25 °C as a function of the solubility parameter of the solvent. Data were taken from the same sources specified for Figures 10–12.

the agreement is actually remarkable, with the data sets for polymers and liquids practically merging.

4. Conclusions

The solubility of carbon dioxide and ethane in a cross-linked poly(ethylene oxide) rubber, as well as the corresponding sorptive dilation of the polymer, was experimentally determined at five different temperatures ($253 \leq T \text{ (K)} \leq 308$) and with a maximum gas pressure of about 21 atm.

The polymer has a strong affinity for carbon dioxide, whose equilibrium concentrations in the polymer at a given operating condition are 1 order of magnitude higher than those of ethane. This affinity, ascribed to the specific interaction of this gas with the ether groups in the polymer chain, leads to a temperature-independent Flory–Huggins interaction parameter and to an unusually high enthalpy of mixing. Ethane, lacking any specific interaction with the polymer, exhibits a temperature-dependent Flory–Huggins parameter, as theoretically expected, and a considerably smaller enthalpy of mixing. For both gases, significant errors in the experimentally determined solubility in the polymer arise if the changes in the volume of the polymer sample due to thermal expansion and gas sorption are not taken into account.

The partial molar volume (PMV) of both carbon dioxide and ethane in the polymer increases with the operating temperature. The corresponding thermal expansion coefficient has the same order of magnitude as the one associated with the pure liquids, although it is somewhat smaller in the polymer than in the liquids. Contrary to the assumption in many prior literature reports, the PMV of a given gas dissolved in a rubbery polymer does depend on the chemical structure of the polymer. This dependence is demonstrated by a decreasing trend of the PMV with increasing solubility parameter of the polymer, a behavior which is also observed in the case of gases dissolved in liquids. Such a trend is interpreted for both matrices (i.e., liquids and polymers) by considering the penetrant to behave like a gas being compressed to its liquid-like volume by the internal pressure of the solvent. Therefore, the use of averages among different liquids and/or different polymers, frequently observed in previous studies of PMVs of gases in polymers, should be avoided when possible. Different materials, either liquids or polymers, at a given temperature, ought to be compared in terms of their solubility parameters, as far as the PMV of a dissolved gas is concerned. For the two gases investigated in this work, PMV data in liquids and rubbery polymers seem to lie on the same curve as a function of the respective solubility parameters,

Table 3. Coefficients⁴⁰ for the Calculation of B (cm^3/mol) Using Eq 17

gas	a_0 (cm^3/mol)	a_1 ($\text{cm}^3 \cdot \text{K}/\text{mol}$)	a_2 ($\text{cm}^3 \cdot \text{K}^2/\text{mol}$)	a_3 ($\text{cm}^3 \cdot \text{K}^3/\text{mol}$)
CO_2	5.7400×10	-3.8829×10^4	4.2899×10^5	-1.4661×10^9
C_2H_6	1.0773×10^2	-8.2548×10^4	5.2387×10^6	-1.9764×10^9

Table 4. Third Virial Coefficients for CO_2 Selected in This Work from the Tables Provided by Dymond et al.⁴⁰

T (K)	C ($10^3 \text{ cm}^6/\text{mol}^2$)	T (K)	C ($10^3 \text{ cm}^6/\text{mol}^2$)
230.00	3916	280.00	5636
240.00	4968	290.00	5236
250.00	5681	298.15	4905
260.00	5819	300.00	4927
270.00	5883	320.00	4423

Table 5. Third Virial Coefficients for C_2H_6 Selected in This Work from the Tables Provided by Dymond et al.⁴⁰

T (K)	C ($10^3 \text{ cm}^6/\text{mol}^2$)	T (K)	C ($10^3 \text{ cm}^6/\text{mol}^2$)
238.77	3704	310.94	8486
254.81	8504	320.00	9641
298.16	10 377	333.15	9030

supporting the hypothesis that gases dissolved in these two kinds of matrices are in a similar thermodynamic state.

Acknowledgment. C.P.R. would like to thank the Brazilian Agency CAPES for their financial support (Grant 2458/07-1). We also gratefully acknowledge partial support of this work by the U.S. Department of Energy (Grant DE-FG02-02ER15362) and by the U.S. National Science Foundation (Grant CBET-0515425). A portion of this research is based upon work supported by the U.S. National Science Foundation under Grant No. DMR #0423914.

Appendix

Gas density was predicted utilizing the virial equation of state truncated to three terms:³⁸

$$Z \equiv \frac{P}{RT\rho} = 1 + B\rho + C\rho^2 \quad (16)$$

where B and C are the second and third virial coefficients, whose values are gas- and temperature-dependent. In the case of B , Dymond et al.⁴⁰ screened available literature values for each gas to fit the following smoothing function of temperature, which was adopted in this work:

$$B(T) = \sum_{i=0}^3 a_i T^i \quad (17)$$

The a_i values for carbon dioxide and ethane are listed in Table 3.

No smoothing function was available in the case of C , though, and the literature values presented by Dymond et al.⁴⁰ were screened in this work by comparison of predicted densities with available literature data.^{41–43} The values of C that led to the smallest mean deviation predictions for each gas are listed in Tables 4 and 5. When the value for a given operating temperature was not available, linear interpolation between the two closest temperatures was employed.

Pure gas fugacity is related to gas density as follows:³⁸

$$\ln \frac{f}{P} = Z - 1 - \ln Z + \int_0^\rho (Z - 1) \frac{d\rho}{\rho} \quad (18)$$

Thus, direct substitution of eq 16 into eq 18 yields:

$$f = P \exp \left(2B\rho + \frac{3}{2}C\rho^2 - \ln Z \right) \quad (19)$$

References and Notes

- (1) EIA, *Annual Energy Review 2006*; Energy Information Administration, <http://www.eia.doe.gov/aer>, 2006.

- (2) Baker, R. W. *Membrane Technology and Application*, 2nd ed.; McGraw-Hill: New York, 2004.
- (3) USDE, *Today's Hydrogen Production Industry*; U.S. Department of Energy, <http://www.fossil.energy.gov/programs/fuels/hydrogen/currenttechnology.html>, 2008.
- (4) Aaron, A.; Tsouris, C. *Sep. Sci. Technol.* **2005**, *40*, 321–348.
- (5) Baker, R. W.; Lokhandwala, K. *Ind. Eng. Chem. Res.* **2008**, *47*, 2109–2121.
- (6) Tabe-Mohammadi, A. *Sep. Sci. Technol.* **1999**, *34*, 2095–2111.
- (7) Baker, R. W. *Ind. Eng. Chem. Res.* **2002**, *41*, 1393–1411.
- (8) Granite, E. J.; O'Brien, T. *Fuel Process. Technol.* **2005**, *86*, 1423–1434.
- (9) Koros, W. J.; Mahajan, R. *J. Membr. Sci.* **2000**, *175*, 181–196.
- (10) Powell, C. E.; Qiao, G. G. *J. Membr. Sci.* **2006**, *279*, 1–49.
- (11) Sridhar, S.; Smitha, B.; Aminabhavi, T. M. *Sep. Purif. Rev.* **2007**, *36*, 113–174.
- (12) Hirayama, Y.; Kase, Y.; Tanihara, N.; Sumiyama, Y.; Kusuki, Y.; Haraya, K. *J. Membr. Sci.* **1999**, *160*, 87–99.
- (13) Patel, N. P.; Miller, A. C.; Spontak, R. J. *Adv. Mater.* **2003**, *15*, 729–733.
- (14) Patel, N. P.; Miller, A. C.; Spontak, R. J. *Adv. Funct. Mater.* **2004**, *14*, 699–707.
- (15) Lin, H.; van Wagner, E.; Raharjo, R.; Freeman, B. D.; Roman, I. *Adv. Mater.* **2006**, *18*, 39–44.
- (16) Lin, H.; van Wagner, E.; Freeman, B. D.; Toy, L. G.; Gupta, R. P. *Science* **2006**, *311*, 639–642.
- (17) Lin, H.; Freeman, B. D. *J. Membr. Sci.* **2004**, *239*, 105–117.
- (18) Lin, H.; Freeman, B. D. *J. Mol. Struct.* **2005**, *739*, 57–174.
- (19) Patel, N. P.; Aberg, C. M.; Sanchez, A. M.; Capracotta, M. D.; Martin, J. D.; Spontak, R. J. *Polymer* **2004**, *45*, 5941–5950.
- (20) Lin, H.; Kai, T.; Freeman, B. D.; Kalakkunnath, S.; Kalika, D. S. *Macromolecules* **2005**, *38*, 8381–8393.
- (21) Raharjo, R. D.; Lin, H.; Sanders, D. F.; Freeman, B. D.; Kalakkunnath, S.; Kalika, D. S. *J. Membr. Sci.* **2006**, *283*, 253–265.
- (22) Lin, H.; Freeman, B. D. *Macromolecules* **2006**, *39*, 3568–3580.
- (23) Patel, N. P.; Hunt, M. A.; Lin-Gibson, S.; Bencherif, S.; Spontak, R. J. *J. Membr. Sci.* **2005**, *251*, 51–57.
- (24) Lin, H.; van Wagner, E.; Swinnea, J. S.; Freeman, B. D.; Pas, S. J.; Hill, A. J.; Kalakkunnath, S.; Kalika, D. S. *J. Membr. Sci.* **2006**, *276*, 145–161.
- (25) Zhao, H. Y.; Cao, Y. M.; Ding, X. L.; Zhou, M. Q.; Yuan, Q. J. *Membr. Sci.* **2008**, *310*, 365–373.
- (26) Lin, H.; Freeman, B. D. *Macromolecules* **2005**, *38*, 8394–8407.
- (27) Kelman, S.; Lin, H.; Sanders, E. S.; Freeman, B. D. *J. Membr. Sci.* **2007**, *305*, 57–68.
- (28) Rajendran, A.; Bonavoglia, B.; Forrer, N.; Storti, G.; Mazzotti, M.; Morbidelli, M. *Ind. Eng. Chem. Res.* **2005**, *44*, 2549–2560.
- (29) Liu, D.; Tomasko, D. L. *J. Supercrit. Fluids* **2007**, *39*, 416–425.
- (30) Gall, G. H.; Sanders, E. S. *Oil Gas J.* **2002**, *100*, 48–55.
- (31) Nordstad, K. H.; Kristiansen, T. K.; Dortmund, D. *Proc. 53rd LRGCC Conf.* **2003**, 251–258.
- (32) Raharjo, R. D.; Freeman, B. D.; Sanders, E. S. *J. Membr. Sci.* **2007**, *292*, 45–61.
- (33) McDowell, C. C.; Coker, D. T.; Freeman, B. D. *Rev. Sci. Instrum.* **1998**, *69*, 2510–2513.
- (34) Bondar, V. I.; Freeman, B. D.; Pinnau, I. *J. Polym. Sci., Part B: Polym. Phys.* **2000**, *38*, 2051–2062.
- (35) Koros, W. J.; Paul, D. R. *J. Polym. Sci., Polym. Phys. Ed.* **1976**, *14*, 1903–1907.
- (36) Lin, H.; Freeman, B. D. Permeation and diffusion. In *Springer Handbook of Materials Measurement Methods*; Czichos, H., Saito, T., Smith, L., Eds.; Springer: Leipzig, 2006; pp 371–397.
- (37) Burnett, E. S. *J. Appl. Mech.* **1936**, *3*, 136–140.
- (38) Van Ness, H. C.; Abbott, M. M. Thermodynamics. In *Perry's Chemical Engineer's Handbook*, 7th ed.; Perry, R. H., Green, D. W., Eds.; McGraw-Hill Professional: New York, 1997; pp 4-1–4-36.
- (39) Koros, W. J.; Paul, D. R.; Rocha, A. A. *J. Polym. Sci., Polym. Phys. Ed.* **1976**, *14*, 687–702.
- (40) Dymond, J. H.; Marsh, K. N.; Wilhoit, R. C.; Wong, K. C. *The Virial Coefficients of Pure Gases and Mixtures*; Springer: Darmstadt, 2001.
- (41) Holste, J. C.; Hall, K. R.; Eubank, P. T.; Esper, G.; Watson, M. Q.; Warowny, W.; Bailey, D. M.; Young, J. G.; Bellomy, M. T. *J. Chem. Thermodyn.* **1987**, *19*, 1233–1250.
- (42) Weber, L. A. *Int. J. Thermophys.* **1992**, *13*, 1011–1032.
- (43) Younglove, B. A.; Ely, J. F. *J. Phys. Chem. Ref. Data* **1987**, *16*, 577–797.
- (44) Liley, P. E.; Thompson, G. H.; Friend, D. G.; Daubert, T. E.; Buck, E. Physical and chemical data. In *Perry's Chemical Engineer's Handbook*, 7th ed.; Perry, R. H., Green, D. W., Eds.; McGraw-Hill Professional: New York, 1997; pp 2-1–2-374.
- (45) Van Krevelen, D. W. *Properties of Polymers*, 3rd ed.; Elsevier: Amsterdam, 1997.
- (46) Matteucci, S.; Yampolskii, Y.; Freeman, B. D.; Pinnau, I. Transport of gases and vapors in glassy and rubbery polymers. In *Materials Science of Membranes for Gas and Vapor Separation*; Yampolskii, Y., Pinnau, I., Freeman, B. D., Eds.; John Wiley & Sons: New York, 2006; pp 1–47.
- (47) Allcock, H. R.; Lampe, F. W.; Mark, J. E. *Contemporary Polymer Chemistry*, 3rd ed.; Pearson Education: Upper Saddle River, 2003.
- (48) Anderson, T. F.; Abrams, D. S.; Grens, E. A. *AIChE J.* **1978**, *24*, 20–29.
- (49) Pinto, J. C. *ESTIMA - A Software for Parameter Estimation and Experimental Design*; Technical Report, **1990**.
- (50) Michaels, A. S.; Bixler, H. J. *J. Polym. Sci.* **1961**, *50*, 393–412.
- (51) Hirose, T.; Mizoguchi, K.; Kamiya, Y. *J. Polym. Sci., Part B: Polym. Phys.* **1986**, *24*, 2107–2115.
- (52) Kamiya, Y.; Naito, Y.; Mizoguchi, K. *J. Polym. Sci., Part B: Polym. Phys.* **1989**, *27*, 2243–2250.
- (53) Kamiya, Y.; Mizoguchi, K.; Hirose, T.; Naito, Y. *J. Polym. Sci., Part B: Polym. Phys.* **1989**, *27*, 879–892.
- (54) Kamiya, Y.; Naito, Y.; Bourbon, D. J. *J. Polym. Sci., Part B: Polym. Phys.* **1994**, *32*, 281–286.
- (55) Wang, J.-S.; Naito, Y.; Kamiya, Y. *J. Polym. Sci., Part B: Polym. Phys.* **1996**, *34*, 2027–2033.
- (56) Merkel, T. C.; Bondar, V.; Nagai, K.; Freeman, B. D.; Yampolskii, Y. P. *Macromolecules* **1999**, *32*, 8427–8440.
- (57) Kamiya, Y.; Naito, Y.; Terada, K.; Mizoguchi, K. *Macromolecules* **2000**, *33*, 3111–3119.
- (58) Tsuboi, A.; Kolar, P.; Ishikawa, T.; Kamiya, Y.; Masuoka, H. *J. Polym. Sci., Part B: Polym. Phys.* **2001**, *39*, 1255–1262.
- (59) Kerbow, D. L.; Sperati, C. A. Physical constants of fluoropolymers. In *Polymer Handbook*, 4th ed.; Brandrup, J., Immergut, E. H., Grulke, E. A., Eds.; John Wiley & Sons: New York, 1997; pp V31–V58.
- (60) Kazarian, S. G.; Vincent, M. F.; Bright, F. V.; Liotta, C. L.; Eckert, C. A. *J. Am. Chem. Soc.* **1996**, *118*, 1729–1736.
- (61) Ham, J. S.; Bolen, M. C.; Hughes, J. K. *J. Polym. Sci.* **1962**, *57*, 25–40.
- (62) Fleming, G. K.; Koros, W. J. *Macromolecules* **1986**, *19*, 2285–2291.
- (63) Kamiya, Y.; Mizoguchi, K.; Terada, K.; Fujiwara, Y.; Wang, J.-S. *Macromolecules* **1998**, *31*, 472–478.
- (64) Kamiya, Y.; Hirose, T.; Naito, Y.; Mizoguchi, K. *J. Polym. Sci., Part B: Polym. Phys.* **1988**, *26*, 159–177.
- (65) Bourbon, D.; Kamiya, Y.; Mizoguchi, K. *J. Polym. Sci., Part B: Polym. Phys.* **1990**, *28*, 2057–2069.
- (66) Pope, D. S.; Sanchez, I. C.; Koros, W. J.; Fleming, G. K. *Macromolecules* **1991**, *24*, 1779–1783.
- (67) Briscoe, B. J.; Zakaria, S. *J. Polym. Sci., Part B: Polym. Phys.* **1991**, *29*, 989–999.
- (68) Briscoe, B. J.; Lorge, O.; Wajs, A.; Dang, P. *J. Polym. Sci., Part B: Polym. Phys.* **1998**, *36*, 2435–2447.
- (69) Angelis, M. G.; Merkel, T. C.; Bondar, V. I.; Freeman, B. D.; Doghieri, F.; Sarti, G. C. *J. Polym. Sci., Part B: Polym. Phys.* **1999**, *37*, 3011–3026.
- (70) Bonavoglia, B.; Storti, G.; Morbidelli, M.; Rajendran, A.; Mazzotti, M. *J. Polym. Sci., Part B: Polym. Phys.* **2006**, *44*, 1531–1546.
- (71) Horiuti, J. *Sci. Pap. Inst. Phys. Chem. Res. (Tokyo)* **1931**, *17*, 125–264.
- (72) Hildebrand, J. H.; Scott, R. L. *Solubility of Non-electrolytes*, 3rd ed.; Reinhold Publ. Corp.: New York, 1950.
- (73) Gjaldabæk, J. C.; Hildebrand, J. H. *J. Am. Chem. Soc.* **1950**, *72*, 1077–1078.
- (74) Masterton, W. L. *J. Chem. Phys.* **1954**, *22*, 1830–1833.
- (75) Ng, W. Y.; Walkley, J. J. *Phys. Chem.* **1969**, *73*, 2274–2278.
- (76) Toppel, E. W.; Gubbins, K. E. *J. Phys. Chem.* **1972**, *76*, 3044–3049.
- (77) Weiss, R. F. *Mar. Chem.* **1974**, *2*, 203–215.
- (78) Moore, J. C.; Battino, R.; Rettich, T. R.; Handa, Y. P.; Wilhelm, E. *J. Chem. Eng. Data* **1982**, *27*, 22–24.
- (79) Handa, Y. P.; D'arcy, P. J.; Benson, G. C. *Fluid Phase Equilib.* **1982**, *8*, 181–196.
- (80) Kamiya, Y.; Naito, Y.; Hirose, T.; Mizoguchi, K. *J. Polym. Sci., Part B: Polym. Phys.* **1990**, *28*, 1297–1308.
- (81) Xu, Y.; Li, L.; Hepler, L. G. *Can. J. Chem.* **1992**, *70*, 55–57.
- (82) Cibulka, I.; Heintz, A. *Fluid Phase Equilib.* **1995**, *107*, 235–255.
- (83) Ashcroft, S. J.; Isa, M. B. *J. Chem. Eng. Data* **1997**, *42*, 1244–1248.
- (84) Grulke, E. A. Solubility parameter values. In *Polymer Handbook*, 4th ed.; Brandrup, J., Immergut, E. H., Grulke, E. A., Eds.; John Wiley & Sons: New York, 1997; pp VII675–VII714.
- (85) Lyckman, E. W.; Eckert, C. A.; Prausnitz, J. M. *Chem. Eng. Sci.* **1965**, *20*, 685–691.
- (86) Smith, E. B.; Walkley, J. *J. Am. Chem. Soc.* **1962**, *66*, 597–599.
- (87) Kamiya, Y.; Terada, K.; Mizoguchi, K.; Naito, Y. *Macromolecules* **1992**, *25*, 4321–4324.
- (88) Charati, S. G.; Stern, S. A. *Macromolecules* **1998**, *31*, 5529–5535.